Copy-Move Forgery Detection using Conjugate Moment Invariants

Hongbo Yang[1,2], Mengmeng Zhou [1*], Jingmin Gao[1,2], Xia Hou[3,4]

1 *School of Automation*, Beijing Information Science and Technology University, Haidian Dist., No.12, QINGHE XIAOYINGDULU, Beijing, China
2 *Electric Information and Control Laboratory Centre*, Beijing Information Science and Technology University, Chaoyang Dist., No.35, BEISIHUAN ZHONGLU, Beijing, China
3 *School of Computer Science,* Beijing Information Science and Technology University, Chaoyang Dist., No.35, BEISIHUAN ZHONGLU, Beijing, China
4 *Beijing Key Laboratory of Internet Culture and Digital Dissemination Research*, Beijing Information Science and Technology University, Chaoyang Dist., No.35, BEISIHUAN ZHONGLU, Beijing, China
* corresponding author's email: *zhouzhou_880118@163.com*

***Abstract* — Copy-move forgery (CMF) is an image operation in which some parts of original image are moved to another location. The purpose of CMF is to hide or add important information to the original image. This paper presents a new CMF detection (CMFD) approach based on conjugate moment invariants (CMIs). The detected image is first divided into overlapping patches, and then the CMIs for each patch are computed. Finally, sorting the computation results is performed to detect all the CMF regions. Unlike common intensity moment invariants, the proposed CMIs include information concerning both image intensity and variations in local intensity (such as the gradient information or the local binary pattern (LBP) information). The proposed method not only has the same invariant properties as the intensity moment invariants but the other advantage in eliminating mismatching and improving matching precision. In addition, the multi-scale CMIs are also designed to overcome the wrong detection due to additive noise and JPEG compression. The experiment-based CoMoFoD database shows that the proposed CMFD method can achieve very excellent detection results.**

Keywords - Conjugate moment invariants (CMIs); Multi-scale; Copy-move forgery detection (CMFD); Intensity moment invariants; Gradient information; LBP information

I. INTRODUCTION

Digital images involve a large amount of information in the digital contents and have widespread applications in various domains [1]. Forgers attempt to tamper with important information from images in order to hide some important fact. Copy-move forgery (CMF) is a frequently used method of image forgery. It is a kind of image operation in which some parts of the original image are moved to another location. CMF can easily match the properties of the duplicated region to the rest of image so that the tempering trace is difficult to notice using the human eye.

Many methods of copy-move forgery detection (CMFD) have been introduced in previous works to identify regions that have been tampered with. Generally, CMFD algorithms can be divided into two categories: blocking methods and key-point extraction methods [2]. The former category usually divides the image into patches and then computes feature descriptors in each patch, finally matching possible similar areas through dictionary sorting comparison. Blocking methods include two schemes: non-overlapping patches and overlapping patches. Because the locations of CMF regions are not known before the process begins, most algorithms use overlapping patches to detect objects pixel-by-pixel. Blocking-based methods are presented in several previous works [3]-[9]. They include DCT [3], moment invariants [4], and PCA [7]. In addition, some pre-processing jobs can increase precision if performed before CMFD. For example, in order to decrease the complexity of the computation, one method segments images into small homogenous patches and performs detection on only those homogenous patches [10].

The other category includes Harris [11], SIFT [12]-[13], and SURF [14]. These methods usually involve searching local corners or key points through the whole image and combining other algorithms to prevent mismatching. These algorithms show reasonable levels of robustness against a wider spectrum of intermediate and post-processing operations than those in the other category. However, they are more complicated and time consuming. Another disadvantage is the inability to detect the copy-move regions that have highly uniform texture. The algorithms also depend heavily on several threshold values [15].

The rest of this paper is organized as follows. Section II summarizes the related works and Section III introduces a new CMFD methods based on conjugate moment invariants

(CMIs). Section IV presents a more efficient and less time-consuming means of implementing the new method. The experimental results are shown in Section V. Section VI discusses the future work and presents the conclusion.

II. RELATED WORKS

In one previous paper, the authors summarized most of the proposed CMFD algorithms and compared their properties, which are listed in Table 1 and Table 2 [10].

TABLE 1. ROBUSTNESS OF TWO CLASSES CMFD ALGORITHMS TO INTERMEDIATE OPERATIONS [15]

	Size of Feature Vector	Robustness to Intermediate Operations		
		Mirror Symmetry	Rotation	Scaling
DCT	Relation to Image Block	×	×	×
Logarithm Transformation	4	√	√	√
Texture and Intensity	7	√	90°, 180°, 270°	×
Key-point Invariants	128	√	√	√
Moment Invariants	4	√	√	×
PCA	6	×	×	×
SVD	Relationship to Threshold	×	×	×

TABLE 2. ROBUSTNESS OF TWO CLASSES CMFD ALGORITHMS TO POST-PROCESSING [15]

	Robustness to Post-processing			Affine Transformation Estimation
	JPEG Compressing	AWGN	Burring	
DCT	×	×	×	×
Logarithm Transformation	√	√	√	×
Texture and Intensity	√	90°, 180°, 270°	×	×
Keypoint Invariants	√	√	√	×
Moment Invariants	√	√	×	√
PCA	×	×	×	×
SVD	×	×	×	×

As shown in Table 1 and Table 2, the moment invariants (MIs) are robust against intermediate and post-processing operations. In addition, MI methods simpler expression and better invariance than other methods. Both these reasons render MIs one of the most important types of methods of CMFD. The Moment method was first presented by Hu in 1962 [16]. It was then called Hu moments (HMs), and it is a traditional kind of MI. HMs were first used in a CMFD by Liu et al. [17]. In Liu's algorithm, HMs had good robustness to post-processing and rotation. Researchers later presented a group of MIs constituting an MI family. For better rotation effects on CMFD, Ryu et al. proposed an algorithm based on Zernike moments [18]. The experimental results showed a higher detection ratio with various rotation degrees than in previous studies [12][14]. However, both HMs and Zernike moments are distorted under discrete conditions

Equation (1) describes the discrete normalized central HMs. The uniform mathematical expression of the (m+n)th order moment in an M × N image can be defined by Equation (2), in which f(x, y) represents intensity function. These intensity MIs are used to describe the image's local invariance properties.

$$M_{pq} = \frac{1}{\sum_{x=1}^{M}\sum_{y=1}^{N} f(x,y)} \sum_{x=1}^{M}\sum_{y=1}^{N} (x-x_0)^p (y-y_0)^q f(x,y) \quad (1)$$

$$M_{pq} = NF \times \sum_{x=1}^{M}\sum_{y=1}^{N} Kernel_{pq}(x,y) \times f(x,y) \quad (2)$$

An intensity MI family is summarized in Table 3. HMs' kernel form is simple and its discretization expression is robust to intermediate and post-processing operations. But the HMs no longer preserve the invariances in digital image.

The improved expressions have been introduced in Section III-A.

Considering that traditional HM methods only preserve invariance properties in the uniform texture images, this paper presents a new passive and overlapping blocking CMFD method using conjugate moment invariants (CMIs). Unlike intensity MIs, the proposed CMIs include both image intensity information and the gradient information or local binary pattern (LBP) information, which describes local

intensity variations. The new image moments CMIs offer some advantages in image operations, such as texture information and blurring.

TABLE 3. MAIN CHARACTERISTICS OF ORTHOGONAL MOMENT FAMILIES [19]

Moment family	Properties		
	Type	Coordinate system	Polynomial form
Hu moments (HMs)	Continuous/ discrete	[-1,1]/image dimensions	$P_m(x)=x^m,\ P_n(x)=x^n$
Zernike moments (ZMs)	Continuous	Unit discpolar coordinates	$R_{mn}(r,\theta)=\left(\sum_{s=0}^{n-\lvert m\rvert/2}(-1)^s\frac{(n-s)!}{s!(n+\lvert m\rvert/2-s)!(n-\lvert m\rvert/2-s)!}r^{n-2s}\right)$
Legendre moments (LMs)	Continuous	[-1,1]	$L_m(x)=\frac{1}{2^m m!}\frac{d^m(x^2-1)^m}{dx^m},$ $L_n(x)=\frac{1}{2^n n!}\frac{d^n(x^2-1)^n}{dx^n}$
Tchebichef moments (TMs)	Discrete	Image dimensions	$t_m(y)=\sum_{k=0}^{m}(-1)^{m-k}\binom{M-1-k}{m-k}\binom{m+k}{m}\binom{y}{k}$ $t_n(x)=\sum_{k=0}^{n}(-1)^{n-k}\binom{N-1-k}{n-k}\binom{n+k}{n}\binom{x}{k}$
Krawtchouk moments (KMs)	Discrete	Image dimensions	$K_m(x;p_1,N)=\sum_{k=0}^{M}a_{k,n,p2}x^k$ $K_n(x;p_1,N)=\sum_{k=0}^{N}a_{k,n,p_i}x^k$

III. CONJUGATE MOMENT INVARIANTS

A. Modified Hu Moment Invariants (HMIs)

HMs are a kind of scalar function. These are used as feature vectors to describe digital images [20]. Using HMs as CMFD descriptors is a robust way to perform specific transformations, such as intermediate operations. However, in the practical application, the properties of traditional HMs distort digital images. For example, the traditional HMs are affected by scaling factors introduced by the following [21].

$$\begin{cases} x = kx' + d \\ y = ky' + d \end{cases} \tag{3}$$

Due to affine transformation, the normalized central moment Mpq has been distorted with scaling and translation, such as in Equation (4).

$$M'_{pq} = k^{p+q} M_{pq} \tag{4}$$

It is necessary to find a new group of Hu moment invariants (HMIs) robust to affine transformation. The modified HMIs are defined using Equation (5).

Here, $\varphi_i\,(i=1,2,...,6)$ is the normalized central moments described in a previous work [22]. The modified HMIs also eliminate redundancies among the initial seven HMs to some extent. In addition, it is necessary normalize HMIs ranging from 0 to 1, and a new group of HMIs can be successfully deduced according to the Equations (6)- (7).

$$\begin{aligned} \phi_1 &= \varphi_2 / \varphi_1^2, \\ \phi_2 &= \varphi_3 / \varphi_1^3, \\ \phi_3 &= \varphi_4 / \varphi_1^3, \\ \phi_4 &= \varphi_5 / \varphi_1^6, \\ \phi_5 &= \varphi_6 / \varphi_1^3, \\ \phi_6 &= \varphi_7 / \varphi_1^6 \end{aligned} \tag{5}$$

$$\phi_i = \left|\lg(\phi_i)^2\right| \tag{6}$$

$$\phi_i = (\phi_i - \phi_{\min}) / (\phi_{\max} - \phi_{\min}), i = 1,2,...6 \tag{7}$$

B. Grey-Grads and Grey-LBP Conjugate Moment Invariants (CMIs)

(a) Results and analysis of intensity-based HMI detection

In part A, one group of HMIs invariant to discrete image is deduced. Using these HMIs to detect CMF regions in the intensity image has achieved good results but it still fails to detect the large, flat regions or blurring images. The corresponding detection results are shown in Fig.(1) and Fig.(2), which indicates that using only intensity-based HMIs is difficult to eliminate mismatching patches in the large flat regions or blurring of the image.

(a) (b) (c)

Fig. (1). Intensity-based HIMs Used to Flat Region Detection
(a) original image; (b) forged image
(c) Detection using intensity-based HIMs

(a) (b) (c)

Fig. (2). Intensity-based HIMs Method Used to Burring Image Detection
(a) original image; (b) blurred image;
(c) detection result image using intensity-based HIMs

(b) grey-grads/grey-LBP CMIs detection results and analysis

To overcome the weakness of intensity-based HMIs, in addition to the intensity information, conjugate invariant moments (CIMs) include the local intensity variations. Local intensity variations have many specific characteristics, such as edge representation and robustness to flat regions tampering or image blurring. In this paper, gradient information and LBP information are used to describe local intensity variations information [27]-[30]. The testing results based on grey-grads or grey-LBP CMIs are shown in Fig.(3) and Fig.(4), which has achieve excellent detection results in flat regions detection and blurring of the image.

(a) (b)

Fig. (3). CIM Methods Used to Detect Flat Regions
(a) gray-grads CMIs method; (b) LBP CMI method

(a) (b)

Fig. (4). CIMs Method Used to Burring Image Detection
(a) gray-grads CMIs method; (b) LBP CMI method.

CMIs are joint HMIs that can be divided into two groups: intensity-based HMIs and local intensity variations based HMIs.

Define the conjugate function $F(x,y)$ as Equation (8) in which intensity function $f(x,y)$ represents real part of the conjugate function and intensity variations(gradient or LBP), $g(x,y)$ represents the imaginary part. Given one digital image, the intensity variation function g(x, y) (∇f / $LBP_{P,R}$ represent gradient and LBP) is described using Equations (9)- (12).

$$F(x,y) = f(x,y) + g(x,y)j \tag{8}$$

$$\nabla f = \frac{\partial f}{\partial x}\hat{x} + \frac{\partial f}{\partial y}\hat{y} \tag{9}$$

$$LBP_{P,R} = \sum_{p=0}^{P-1} s\left(g_p - g_c\right) \times 2^p \tag{10}$$

with

$$s\left(g_p - g_c\right) = \begin{cases} 1, & g_p - g_c \geq 0 \\ 0, & g_p - g_c < 0 \end{cases} \tag{11}$$

$$LBP_{P,R}^{riu2} = \begin{cases} \sum_{p=0}^{P-1} s\left(g_p - g_c\right) if U\left(LBP_{P,R}\right) \leq 2 \\ \left(P+1\right) otherwise \end{cases} \tag{12}$$

Equations (10) and (11) describe the basic LBP operator, and provide a novel means of analyzing intensity variations, but it is insensitive to illumination and greyscale variations [31]. There is an additional need to enhance its operation by making it invariant to rotation. A rotation invariant LBP operator is described using Equation (12) [32][33].

Eventually, the HMIs computing of $F(x,y)$ can be computed using that of $f(x,y)$ and $g(x,y)$ as follows.

$$M_i = M_{f_i} + M_{g_i} \cdot j \tag{13}$$

Here, Mi represents the conjugate invariant moments, M_{f_i}, M_{g_i} $(i = 1,2,...,6)$ represent the HMIs of intensity information and the HMIs of local intensity variations information, respectively. Here, both M_{f_i} and M_{g_i} are calculated using Equation (5)-(7).

Having calculated the CMIs of each patch, a sorting approach was used to put possibly similar patches together. Then every n adjacent CMI (in this paper, n = 5) was placed in one group. The existence of any similar patches in each group was determined using the specific similarity principle. Here, the minimum Euclidean distance served as the similarity principle. If the Euclidean distance is below a setting threshold (*thre* ≤ 0.5), the compared patches are considered similar to each other. The concrete sorting approach is described as follows.

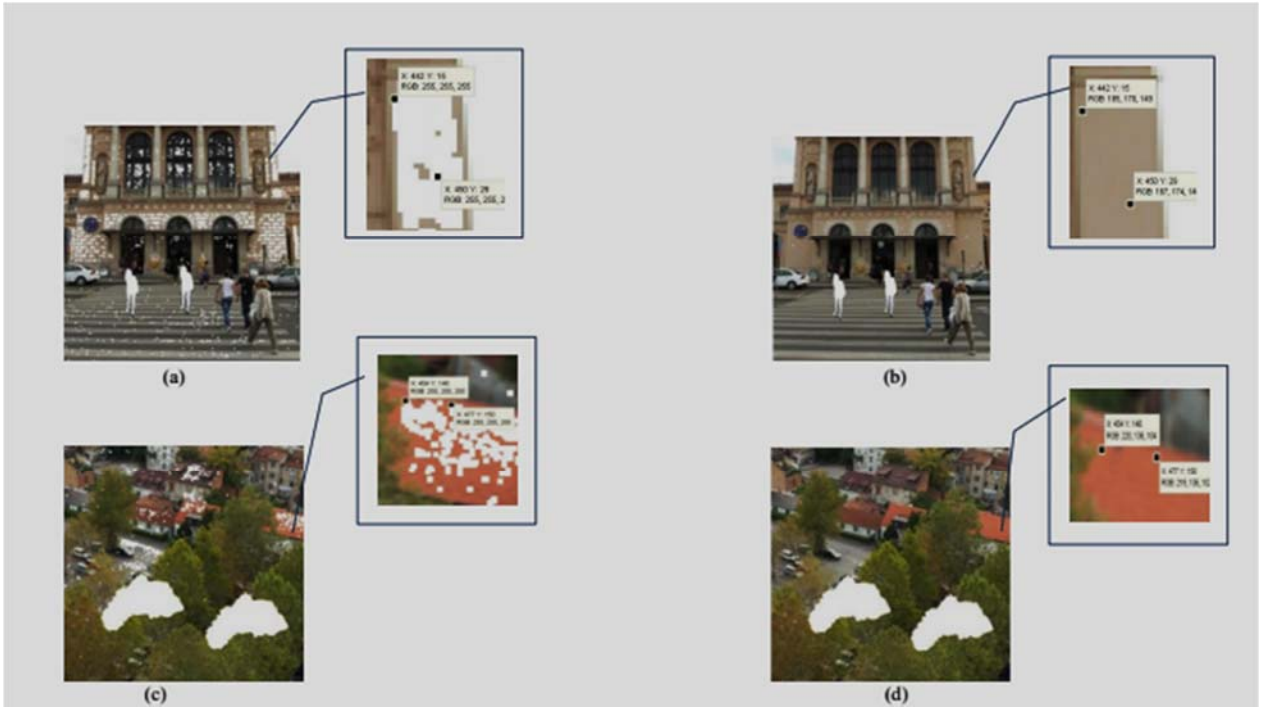

Fig. (5). Detection Results: subfigures (a) and (b) correspond to the same forged image.

After dividing the image into overlapping blocks, the MIs of each patch are realigned to a row vector and then all these MIs vectors are sorted. The method sorts the vectors based on the first value of each MIs vector. For these MIs having equal first value, sorting is based on the next value in vectors until comparing all vectors' elements orderly. The components of the new array are sorted from low to high before use.

(c) CMFD based illustration

Parts (a) and (b) show analysis of the intensity MIs and the CMIs mechanism. Next, the concrete detecting implementation is introduced: (1) sorting all the patches depending on MIs sorting method; (2) grouping every n adjacent MIs (generally, n = 5) into a unit; (3) comparing the similarity of the n adjacent patches' MIs in each unit according to similarity principle; (4) labelling similar patches.

The results of detection are shown in Fig.(5): subfigures (a) and (c) show the detection results based on intensity MIs in two different images. A few mismatched patches are illustrated. Subfigures (b) and (d) show a CMI-based detection method. Then the CMIs of mismatched patches corresponding to (a) and (c) are calculated.

In subfigure (a), the pair of mismatched patches in the top-left corner coordinates are (442, 15) and (450, 29) (their similarity of intensity MIs is 0.0474); and in subfigure (c), the pair of mismatching patches in the top-left corner coordinates are (454, 148) and (477, 150) (their similarity of intensity MIs is 0.0004). Both of these satisfy the setting threshold range (thre $\leq$ 0.5). The computing results show that the similarities of their CMIs to be 1.759 and 2.147 in (b) and (d), respectively, which both them go far beyond the maximum thre (max_thre = 0.5).

The selected two patches' top-left coordinates are (442, 15) and (450, 29) in both subfigures (a) and (b).Subfigure (a) shows the use of the intensity MI method to calculate the similarity of the patches, 0.0474. Subfigure (b) shows calculation of the same pair of patches using the CMI method, 1.795. Selecting a pair of patches and calculating the similarity: in subfigure (c), the similarity of patches as indicated using MI to be 0.0004 (the top-left coordinates are (454, 148) and (477, 150)); and in subfigure (d), the similarity CMI of the same patches is 2,147.

In addition, there are the other non-detectable problems in the testing process. Because it is an image moment, CMIs are sensitive to additive noise and JPEG compression. Multi-scale CMIs are designed to operate these conditions and overcome this weakness.

C. Multi-scale CMIs

In a CMF image, aside from the intermediate operations such as geometric transformation, various post-processing operations are used to make the tampered image look more natural. Some of these post-processes change the image characteristics. In this way, the CMI properties of original and duplicated regions cease to be similar. For example, additive noise is randomly added to the image, and JEPG compression uses sampling and quantization to process the image, both belong to this kind of post-processing. In this way, multi-scale CMIs are used to solve additive noise and JPEG compression images. A Gaussian pyramid basis multi-scale space is described in Fig.(5).

The Gaussian pyramid includes different octaves of different sizes, and each octave consists of different scale images (called levels). Because various scale images (levels) in the same octave have basically the same post-processing characteristics, the CMIs of adjacent levels within the same octave can be calculated, and then all patches on the adjacent levels can be placed together for later sorting. That is, the initial region must be matched in one scale level with the duplicated region in another scale level within the same octave. The same operations can be performed on the other octaves. The multi-scale CMI method is used to search similar regions using matching between different levels in each octave of scale space. This method takes full advantage of CMI robustness to scale blurring and has the same post-processing characteristics in different scale levels of same octave. The multi-scale space is built as follows.

First, the multi-scale space of an image can be defined using expressions (14) and (15). G(x, y, σ) is a variable-scale Gaussian factor, I(x, y) is a digital image.σ represents scale factor.

$$L(x,y,\sigma)=G(x,y,\sigma)*I(x,y) \tag{14}$$

$$G(x,y,\sigma)=\frac{1}{2\pi\sigma^2}e^{-(x^2+y^2)/2\sigma^2} \tag{15}$$

Multi-scale Gaussian kernels described in Equation (16) convolving with image to produce scale space images were used [23]-[26].

$$2^{i-1}\left(k\sigma,k^2\sigma,...,k^{n-1}\sigma\right),k=2^{1/s} \tag{16}$$

According to the multi-scale space definition, the corresponding scale space images can be determined using three steps: building the image's Gaussian pyramid, smoothing the image, and grouping. An efficient approach to constructing scale space images is shown in Fig.(6).

The multi-scale CMIs method searches for similarity in all patches of differently scaled images. Scale images in the first octave have more detailed information than those in the other octave. Testing first detects similar regions between levels in first octave, and then goes on in the smaller octaves, in which detailed information has been lost and images have become flat. This method is meant to detect CMF regions accurately and eliminate mismatched patches.

The set of scale factors is $\{2^{1/3}\sigma,2^{2/3}\sigma,2^{3/3}\sigma\}$, $k=2$, $s=3,\sigma=9$.This satisfies criteria of similar blocks and coordinate relations. Similar regions are labelled with one gray value. This process is performed on the next octave and the next until the final one is processed.

Then down sample method was used to produce a set of scale space images, which grouped them into different octaves (3 octaves are illustrated in Fig.(1)). The first image of each octave is produced by down sampling the largest-scale image of the previous octave. For each octave of scale space, the initial image is repeatedly convolved with Gaussian factors to produce the set of scale space images.

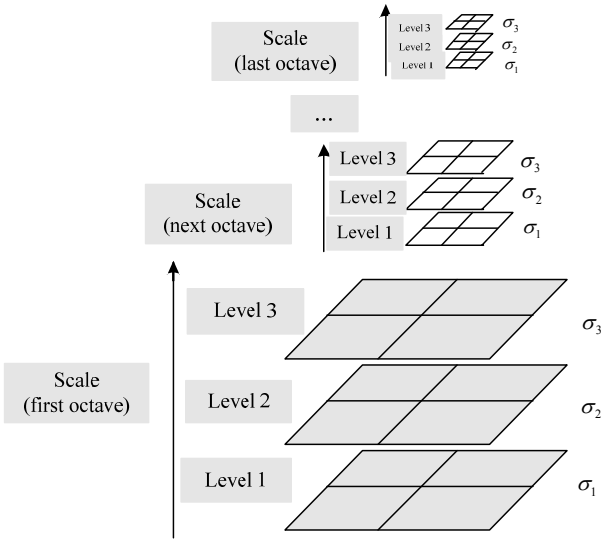

Fig. (6). Gaussian-Pyramid-based Multi-Scale Space:

IV. IMPLEMENTATION

A. Matrix-based Algorithm Design

In this paper, CMI detection depends on blocking methods, which are used to divide the duplicated image into small, overlapping blocks. An *M*×*N* image is divided into overlapping blocks of size *h*×*w*. Because sliding by pixels requires a great deal of time, we present a fast algorithm of dividing blocks based on matrix. First, the *M*×*N* image is divided into *h*×*w* blocks and produces $(N-h+1)\times(M-w+1)$ overlapping blocks. Each *h*×*w* block is rearranged into a column vector. Given one matrix, its row number is *h*×*w* and column number is

$(N-h+1)\times(M-w+1)$. All overlapping blocks constitute the matrix in which each overlapping block is one column.

Depending on matrix-based blocking method, CMIs are calculated for each column in the matrix using Equation (13). $\tilde{M}_{fB}$ and $\tilde{M}_{gB}$ describe the HMIs based on intensity function and intensity variations function, respectively. They are defined as follows.

$$\tilde{M}_B = \left[\tilde{M}_{fB},\ \tilde{M}_{gB}\right] \tag{17}$$

$$\tilde{M}_{fB} = \begin{pmatrix} \tilde{M}_{fb11} & \cdots & \tilde{M}_{fb(M-width+1)\times(N-height+1)1} \\ \vdots & \ddots & \vdots \\ \tilde{M}_{fb16} & \cdots & \tilde{M}_{fb(M-width+1)\times(N-height+1)6} \end{pmatrix} \tag{18}$$

$$\tilde{M}_{gB} = \begin{pmatrix} \tilde{M}_{gb11} & \cdots & \tilde{M}_{gb(M-width+1)\times(N-height+1)1} \\ \vdots & \ddots & \vdots \\ \tilde{M}_{gb16} & \cdots & \tilde{M}_{gb(M-width+1)\times(N-height+1)6} \end{pmatrix} \tag{19}$$

represent six HMIs from each column vector (block) based on intensity function, as with the intensity variation function.

B. Procedure of The Proposed Algorithm

An M×N image has been divided into overlapping blocks, and then a fast algorithm was used to calculate the values of matrix-based CMIs. This process depended on similarity principle for similar blocks detection. The Table 4 details of the proposed algorithm's procedure are shown in Table .

TABLE 4. PROCEDURE OF PROPOSED ALGORITHM

Algorithm 1 the blocking procedure

```
OrigImg = imread();
ImgGray = rgb2gray(OrigImg);
Intensity_Img = double(ImgGray);
%---------- ImgGredient /LBP represents intensity variations information----------%
IntensityVar_Img = ImgGredient(ImgGray);
% IntensityVar_Img = LBP(ImgGray);
[M,N] = size(IntensityVar_Img);
w = 5;
h = 5;
Intensity_matrix = im2col(Intensity_Img, [w,h], 'sliding');
IntensityVar_matrix = im2col(IntensityVar_Img, [w,h], 'sliding');
[col_bar, row_bar] = meshgrid(1:N, 1:M);
col_matrix = im2col(col_bar, [w,h], 'sliding');
row_matrix = im2col(row_bar, [w,h], 'sliding');
HMIs_intensity = HMIs(Intensity_matrix, col_matrix, row_matrix);
HMIs_intensityVar = HMIs(IntensityVar_matrix, col_matrix, row_matrix);
CMIsmatrix = CMIs(HMIs_intensity, HMIs_intensityVar);
```

Algorithm II the similar patches comparison procedure

```
CMIs_sort = sortrows(CMIsmatrix);
N = 5;
Img_forgery = block_cmp(OrigImg, CMIs_sort, N, width, height);
figure
ImgResult = uint8(Img_forgery);
Imshow(ImgResult);
```

V. RESULTS OF TESTING

In this paper, experiments were performed using the CoMoFoD database [27], which is a public benchmark database using for copy-move forgery detection. Images in this database were divided into 5 groups using the applied manipulation: 1. copies from the same region copies; 2. copies from different regions; 3. photometric transformation; 4. rotation; 5. multiple attacks.

Here, 500 images were selected from the CoMoFoD contain above operations. For all tested cases, the following setup was used: converting images into grayscale space; block size was set to 5×5; threshold *thre* = 0.5; removal of falsely detected areas depends using the similarity principle.

The corresponding detection results are shown in Fig.(7) and Fig.(8) and then a time-consuming comparison of different methods was performed and is here discussed. The identification numbers (a)-(d) represent the original image, tampered image, gray-grad basis CMI detection method, and gray-LBP basis CMI detection method.

(a) (b) (c) (d)

Fig. (7). Same Region Multi-Copies

(a) (b) (c) (d)

Fig. (8). **C**opies from Different Regions

The photometric transformation described in CoMoFoD database include color reduction (CR), contrast adjustments (CA), and changes in brightness (BC). The related parameter settings are introduced in Table 5.

TABLE 5. PARAMETER SETTINGS OF POST-PROCESSING FORGERIES

BC	(lower bound, upper bound)		
	(0.01, 0.95)	(0.01, 0.9)	(0.01, 0.8)
CR	Intensity levels per color channel		
	32	64	128
CA	(lower bound, upper bound)		
	(0.01, 0.95)	(0.01, 0.9)	(0.01, 0.8)

A subset of parameter settings was selected to show the testing results (the selected parameters shown in Table 6 Tampered images and test results are shown in Fig.(9)and Fig.(10).

TABLE 6. SUBSET OF PARAMETER SETTINGS

Post-processing parameter		Tampering operation
BC	(lower bound, upper bound)	Distortion + BC
	(0.01, 0.95)	
CA	(lower bound, upper bound)	Translation+ CA
	(0.01, 0.95)	

(a) (b) (c) (d)

Fig. (9). Distortion + BC Detection

(a) (b) (c) (d)

Fig. (10). Translation + CA Detection

The photometric transformation test results showed the CMI-based detection method to be robustness against photometric transformation, blurring, and other problems. The results shown in Fig. 9 show that legs of the duplicated girl were not detected using the grey-grad CMI method but the grey-LBP CMI method was used to detect them perfectly. Thus, compared to gradient, LBP function has a stronger ability to describe variations in intensity.

To detect additive noise and JPEG compression images, multi-scale space must be added to the CMI method.

Experiments showed the expected results.

Setting parameters of added noise (NA) and JPEG compression (JC) based on Table 7 are listed in Fig.(11)and Fig.(12).

TABLE 7. SUBSET OF PARAMETER SETTINGS

JC	Quality factor	Tampering operation
	30	Translation + JC
NA	Averaging filter	Rotation + NA
	3×3	

(a) (b) (c) (d)

Fig. (11). Translation + JC Detection

(a) (b) (c) (d)

Fig. (12). Rotation + NA Detection

This technology is takes advantage of the smaller time requirements of the CMFD algorithms. The runtimes of the novel methods based on grey-grads and grey-LBP

CMIs are listed in Table 8. A comparison of the testing to those of other methods is shown in Table 9, in which the average runtime is listed for 512×512 image. In the view of average runtime, the proposed method has an obvious advantage over the others.

TABLE 8. TIME-CONSUMING COMPARISON OF NOVEL METHODS

Duplicated operator	Average runtime (s)	
	grey-grads	grey-LBP
Geometric transformation	5.6211	5.8471
Photometric transformation	5.8091	5.8911
JC	15.3271	16.021
NA	15.409	16.380

TABLE 9. AVERAGE RUN TIME OF EACH METHOD FOR 512×512 IMAGES

	Detection operator					
	block-based					SIFT-based
	Proposed	uLBP [28][29]	CRLBP [28][30]	Zernike-Moments [31]	DCT [32]	SIFT [33]
Runtime (s)	6	25	27	342	1115	10

VI. CONCLUSIONS

A novel methodology for CMFD is proposed in this paper. The presented method includes both intensity information and intensity variation information. The processing on the multi-scale space is also robust against additive noise and JPEG compression. As a result, the proposed CMFD method produces excellent detection results for geometric transformation forgeries, and it is robust against image post-processing, additive noise, and JPEG compression.

The experiments demonstrate the proposed CMIs method faster than [28]-[34]. However, in bock processing, the current method can fail to scale. In those cases, many blocks are falsely detected alongside duplicated regions. To solve this issue, different scale windows must be used to search for duplicated regions. A better representation of blocking method and feasibility analysis should be presented.

ACKNOWLEDGMENTS

This work was financially supported by the Importation and Development of High-caliber Talents Project of Beijing Municipal Institutions (CIT&TCD201304115) and the Importation and Development of High Caliber Talents Project of Beijing Municipal Institutions (CIT&TCD201504056).

REFERENCES

[1] B. L. Shivakumar and S. S. Baboo, "Detecting copy-move forgery in Digital images: A survey and analysis of current methods", Global Journal of Computer Science and Technology, 2010, 10(7): 61-65.

[2] V. Christlein, C. Riess, J. Jordan, C. Riess, and E. Angelopoulou, "An evaluation of popular copy-move forgery detection approaches", IEEE Trans. Inf. Forensics Security, 2012, 7(6): 1841–1854.

[3] Y. Huang, W. Lu, W. Sun, and D. Long, "Improved DCT-based detection of copy-move forgery in images", Forensic science international, 2011, 206(1–3): 178–184.

[4] S. Ryu, M. Lee, and H. Lee, "Detection of Copy-Rotate-Move Forgery using Zernike Moments", Information Hiding Conference: IH'10 Proceedings of the 12th international conference on Information hiding. SPRINGER HEIDELBERG: Springer Berlin Heidelberg, 2010: 51-65.

[5] H. Farid and S. Lyu, "Higher-order wavelet statistics and their application to digital forensics", in Proc. IEEE Workshop on Statistical Analysis in Computer Vision (in conjunction with CVPR), Madison, WI, 2003.

[6] Y. Cao, T. Gao, L. Fan, and Q. Yang, "A robust detection algorithm for copy-move forgery in digital images", Forensic Science International, 2012, 214(1–3): 33–43.

[7] A. J. Fridrich, B. D. Soukal, and A. J. Lukáš, "Detection of copy-move forgery in digital images," in Proc. Digit. Forensic Res. Workshop, 2003.

[8] S. Bayram, H. T. Sencar, and N. Memon, "An efficient and robust method for detecting copy-move forgery", in Proc. IEEE Int. Conf. Acoust., Speech Signal Process. (ICASSP), Washington, DC, USA, 2009: 1053–1056.

[9] M. Zimba, S. Xingming, Fast and robust image cloning detection using block characteristics of DWT coefficients, Int. J. Digital Content Technol. Appl, 2011, 5 (7): 359–367.

[10] Jian Li, Xiaolong Li, Bin Yang, and Xingming Sun, "Segmentation-Based Image Copy-Move Forgery Detection Scheme", IEEE Trans. Inf. Forensics Security, 2015, 10(3): 507–517.

[11] Qiu Jianguo, Zhang Jianguo, Li Kai. An Images Matching Method Based on Harris and Sift Algorithm [J]. Journal of Test and Measurement Technology, 2009, 23 (2): 271-274.

[12] Irene Amerini, Lamberto Ballan, et al, "Geometric tampering estimation by means of a SIFT-based forensic analysis", Acoustics Speech and Signal Processing(ICASSP), 2010 IEEE International Conference on, 2010:1702-1705.

[13] Amerini I, Ballan L, Caldelli R, et al, "A SIFT-based forensic method for copy-move attack detection and transformation recovery", Information Forensics and Security, IEEE Transactions on, 2010, 6(3):1099-1110.

[14] Xu B, Wang J, Liu G, et al, "Image copy-move forgery detection based on SURF", Multimedia Information Networking and Security MINES, 2010 International Conference on, IEEE, 2010: 889-892.

[15] Shivakumar B L, Santhosh Baboo S, "Detection of region duplication forgery in digital images using SURF", International Journal of Computer Science Issues IJCSI, 2011, 8(4).

[16] G.A. Papakostas, D.E. Koulouriotis, E.G. Karakasis, Computation strategies of orthogonal image moments: a comparative study, Appl. Math. Compute, 2010 216 (1): 1–17.

[17] S. Bravo-Solorio and A. K. Nandi, "Exposing duplicated regions affected by reflection, rotation and scaling", in Proc. IEEE Int. Conf. Acoust., Speech Signal Process (ICASSP), 2011: 1880–1883.

[18] Perona P, Malik J, "Scale space and edge detection using anisot ropic diffusion", IEEE Trans Pattern Anal Mach Intell, 1990, 12 (7): 629 - 639.

[19] J I Shu-fang et al, "Face Recognition Based on Gray and Grads Invariant Moments", Journal of Southern Yangze University (Natural Science Edition), 2006, 5 (6): 666 – 669

[20] J Z. He, W. Lu, W. Sun, and J. Huang, "Digital image splicing detection based on Markov features in DCT and DWT domain", PatternRecognition,http://dx.doi.org/10.1016/j.patcog.2012.05.014 .

[21] Sporring, Jon et al. (Eds), "Gaussian Scale-Space Theory, Kluwer Academic Publishers", 2003.

[22] T.Lindeberg, "Scale-space theory: A basic tool for analyzing structures at different scales". Journal of Applied Statistics (2): (Supplement on Advances in Applied Statistics: Statistics and Image, 21 224-270.

[23] Witkin, A.P, "Scale-space filtering", Proc. 8th Int. Joint Conf. Art. Intell., Karlsruhe, Germany, 1983: 1019 – 1022.

[24] Lindeberg, T, "Scale-Space Theory in Computer Vision, Kluwer Academic Publishers", 1994.

[25] Lindeberg, T, "Generalized Gaussian scale-space axiomatic comprising linear scale-space", affine scale-space and apatio-temporal scale-space, Journal of Mathematical Imaging and Vision, 2011, 40(1): 36 – 81.

[26] Lindeberg. T, "Generalized Gaussian axiomatic scale-space theory", Advances in Imaging and Electron Physics, Elsevier, 2013: 178, 1 – 96.

[27] Dijana Tralic, et al, "CoMoFoD – New Database for Copy-Move Forgery Detection", 55th International Symposium ELMAR, IEEE, 2013.

[28] Li Z., Liu G., and You J., "Scale and rotation-invariant local binary pattern using scale-adaptive texture", Proceedings of the IEEE, 2012,67(5): 2130-2140

[29] Leida Li, Shushang Li, Hancheng Zhu, "An efficient Scheme for Detecting Copy-move Forgered Images by Local Binary Patterns", Journal of Information Hiding and Multimedia Signal Processing, Volume 4, Number 1, January 2013, 4(1): 46-56.

[30] Salam Abdul-Nabi Thajeel, et al, "A Novel Approach for Detection of Copy Move Forgery using Completed Robust Local Binary Pattern", Journal of Information Hiding and Multimedia Signal Processing, 2015, 6(2): 351-362.

[31] Seung-Jin Ryu et al, "Rotation Invariant Localization of Duplicated Image Region Based on Zernike Moments", IEEE transactions on information forensics and security, 8(8), 2013: 1355-1370.

[32] Y. Huang, W. Lu, W. Sun, and D.Long, "Improved DCT-based detection of copy-move forgery in images", Forensic Sci.Int, 2011, 206(1-3): 178-184.

[33] X. Pan and S.Lyu, "Region duplicated detection using image feature matching", IEEE transactions on information forensics and security, 2010, 5(4): 857-867.